First published in:

ADVANCED MATERIALS

DOI: 10.1002/adma.200501674

New Route to Three-Dimensional Photonic Bandgap Materials: Silicon Double Inversion of Polymer Templates**

By *Nicolas Tétreault*, *Georg von Freymann*, *Markus Deubel*, *Martin Hermatschweiler*, *Fabian Pérez-Willard*, *Sajeev John*, *Martin Wegener*, and *Geoffrey A. Ozin**

In the quest for three-dimensional photonic crystals[1,2] with omnidirectional photonic bandgaps (PBGs), pioneering "top–down" and "bottom–up" approaches have been explored. The former have led to excellent quality photonic crystals; however, fabrication efforts and costs are high.[3–5] The latter, using colloidal crystals as templates, provide photonic crystals; however, their crystal structure is limited to face-centered cubic and quality is compromised by defects.[6–8] More recent approaches founded on holographic laser lithography[9,10] and direct laser writing in polymer photoresists[11–16] have turned out to fulfill most of the necessary requirements[17] for large-scale fabrication of three-dimensional (3D) photonic crystals, facilitating straightforward incorporation of functional defects like waveguides and resonators.[18] Unfortunately, a major obstacle must be overcome before the way is clear to photonic bandgap materials; namely, polymer templates have insufficient refractive-index contrast to open a complete photonic bandgap. In this report, we overcome these problems by employing a novel, versatile, scalable, and cost-effective silicon double-inversion method to synthesize the first Si replica of a polymeric photonic crystal. This method can be applied to any photoresist template produced by direct-laser writing (DLW), holographic laser lithography, or combinations thereof. It also incorporates a template-independent step to fine-tune the filling fraction of the high-index material, thereby allowing larger PBGs to be obtained than with the template alone. The procedure exclusively comprises straightforward, inexpensive, industry-compatible steps, perfectly suitable for mass production of complex and functionalized photonic-crystal-based devices.

The silicon double inversion is exemplified using the familiar “woodpile” (or log pile) structure to allow direct comparison with “top–down” photonic crystals reported previously.[3–5] The Si woodpile, obtained following the steps shown schematically in Figures 1a–f and detailed hereafter, is 24 layers thick and has a calculated PBG of 8.6 %.

We begin with a polymer woodpile fabricated in the commercially available negative photoresist EPON SU-8. In brief, 120 fs pulses at 800 nm wavelength, derived from a regeneratively amplified Ti:sapphire laser, are focused into the photoresist using a high numerical aperture ($NA = 1.4$) oil-immersion microscope objective. Due to the high intensities in the focal volume, two-photon absorption initiates the polymerization process, resulting in exposed ellipsoidal volume elements (voxels) with a minimum lateral diameter down to 150 nm and a ratio of 2.7 between axial and lateral dimensions after development. Such voxels form the basic building blocks for all 3D structures that can be fabricated by sequentially scanning the laser focus through the resist using a computer-controlled 3D piezo scanning stage, synchronized with the laser pulses. Functional defects like resonators and waveguides can easily be incorporated into the structure. The woodpile structure can be described by successive layers of ellipsoidal rods rotated 90° relative to each other with their second nearest-neighbor layers displaced by $a/2$, where a is the in-layer rod distance. Four layers form a lattice constant c. For $(c/a)^2 = 2$, this 3D lattice exhibits face-centered cubic translational symmetry with a two-rod basis and can be derived from a diamond lattice by replacing the (110) chains of lattice points with rods.[19] For band diagram calculations, the woodpile structure is described by ellipsoidal rods of infinite length with

[*] Prof. G. A. Ozin, N. Tétreault, Dr. G. von Freymann
Materials Chemistry Research Group, Department of Chemistry
University of Toronto
80 St. George Street, Toronto, ON M5S 3H6 (Canada)
E-mail: gozin@chem.utoronto.ca
Dr. G. von Freymann, M. Deubel, M. Hermatschweiler,
Prof. M. Wegener
Institut für Angewandte Physik
and DFG-Center for Functional Nanostructures (CFN)
Universität Karlsruhe
D-76128 Karlsruhe (Germany)
Dr. G. von Freymann, M. Deubel, M. Hermatschweiler,
Prof. M. Wegener
Institut für Nanotechnologie
Forschungszentrum Karlsruhe in der Helmholtz-Gemeinschaft
D-76021 Karlsruhe (Germany)
Dr. F. Pérez-Willard
DFG-Center for Functional Nanostructures (CFN)
Universität Karlsruhe
D-76128 Karlsruhe (Germany)
Prof. S. John
Department of Physics, University of Toronto
60 St. George Street, Toronto, ON M5S 1A7 (Canada)

[**] GAO and SJ are Government of Canada Research Chairs in Materials Chemistry and Physics, respectively. They are indebted to the Natural Sciences and Engineering Research Council of Canada for support of this research. NT is grateful for financial support of his research in the form of a F.E. Beamish Graduate Scholarship (OGSST). The Karlsruhe team acknowledges support by the Deutsche Forschungsgemeinschaft through subproject A1.4 of the DFG-Forschungszentrum “Functional Nanostructures” (CFN) and by projects We 1497/9–1 and Fr 1671/2–1.

EVA-STAR (Elektronisches Volltextarchiv – Scientific Articles Repository)
http://digbib.ubka.uni-karlsruhe.de/volltexte/1000010958
© 2006 WILEY-VCH Verlag GmbH & Co. KGaA, Weinheim
WILEY InterScience DISCOVER SOMETHING GREAT

ADVANCED MATERIALS

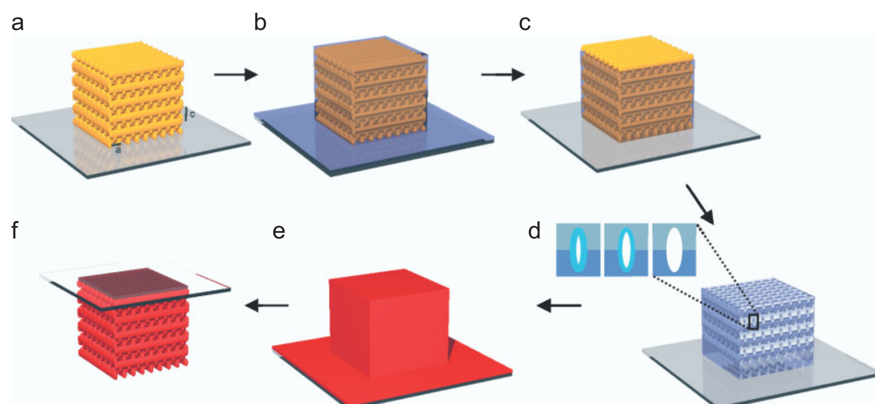

Figure 1. Schematic representation of the silicon double inversion method. a) The SU-8 template is fabricated by DLW. b) Full SiO_2 infiltration by way of layer-by-layer chemical vapor deposition (CVD). c) Anisotropic reactive-ion etching of the top SiO_2 overlayer to uncover the SU-8. d) Removal of the SU-8 template by O_2 plasma etching or calcination in air to obtain the SiO_2 inverse woodpile; inset: re-infiltration of the SiO_2 inverse woodpile by SiO_2 CVD to fine-tune the rod filling fraction. e) Si infiltration of the inverse woodpile by low-pressure CVD. f) Attachment to an HF-resistant substrate with a polymer adhesive and removal of SiO_2 inverse woodpile and substrate by chemical etching in an aqueous HF solution to obtain the Si woodpile replica.

a fixed height (R_y/a) to width (R_x/a) ratio of 2.7. The filling fraction (*ff*) is varied by the parameter R_x/a (rod width/rod spacing). The high optical quality of the templates is demonstrated elsewhere.[13,16] Here we demonstrate double inversion on a 24 layer woodpile of lateral dimensions of 100 μm × 100 μm with a rod spacing of $a = 1.0$ μm and a filling fraction of $ff = 47$ %, which is equivalent to a rod width of $R_x/a = 0.30$ (SU-8 refractive index $n_{SU\text{-}8} = 1.57$).

The first step of the silicon double inversion involves complete infiltration of the SU-8 woodpile (Fig. 1a) by room-temperature atmospheric pressure SiO_2 chemical vapor deposition (CVD).[20] This involves sequential saturation of the template surfaces with water and reaction with $SiCl_4$ (N_2 is used as carrier gas) to deposit amorphous SiO_2 in a layer-by-layer fashion while releasing the silica condensation/polymerization catalyst HCl. The sequence is repeated (on average 10–12 times) until the woodpile is completely infiltrated (Fig. 1b). After CVD infiltration, a thick layer of SiO_2 completely covers the external surfaces of the woodpile template, inhibiting removal of the SU-8. This overlayer is removed by anisotropic reactive-ion etching (RIE) in an SF_6 plasma for 15–30 min to expose the SU-8 structure (Fig. 1c). The SU-8 woodpile is then selectively removed using O_2 plasma etching (for $t > 20$ h) or calcination in air at 450 °C ($t > 6$ h). This reveals the SiO_2 inverse of the original SU-8 structure (Fig. 1d). At this point, we observe a structural shrinkage of 6–7 % after removal of the SU-8 template, which reduces the rod distance and the filling fraction to $a = 940$ nm and $ff = 47$ %, respectively ($R_x/a = 0.28$). This is due to evaporation of encased H_2O molecules which did not react with $SiCl_4$ to form SiO_2 during the CVD. Figure 2a shows a cross-sectional scanning electron microscopy (SEM) image of a SiO_2 inverse woodpile obtained by focused ion beam (FIB) milling of the structure.

The air-rod diameter clearly determines the silicon-rod diameter, and hence the width of the photonic bandgap of the final structure. Therefore, an important step is to precisely control the air-rod diameter to maximize the resulting photonic bandgap. To do so, the SiO_2 inverse woodpile is re-infiltrated using SiO_2 CVD to achieve a desired filling fraction, as shown in Figure 2b. In Figure 2c, one can observe a monotonic red-shift of the SiO_2 inverted woodpile reflectance peak as the air-rod width is reduced from 260 nm ($R_x/a = 0.28$) to 235 nm ($R_x/a = 0.25$) and then 205 nm ($R_x/a = 0.22$). The corresponding calculated PBG evolves from 4.6 % to 8.6 % for Si filling fractions *ff* of 42 % and 27 %, respectively (Fig. 2d).

Finally, the SiO_2 inverse woodpile is infiltrated by Si low-pressure CVD using disilane (Si_2H_6) as precursor ($T = 460$ °C, $p = 3.12$ mbar (1 mbar = 100 Pa), $t = 40$ min).[21] Deposition is stopped when the pores are completely infiltrated, at which point the Si covers the entire SiO_2 inverse woodpile and the glass substrate (Fig. 1e). The Si/SiO_2 composite is then attached to a sapphire substrate using a transparent polymer adhesive. Subsequent chemical wet etching in 2 vol.-% aqueous HF selectively removes the glass substrate and the SiO_2 inverse woodpile. The resulting high-quality hydrogenated amorphous silicon (a-Si:H) woodpile is a near-identical replica of the original SU-8 woodpile (Fig. 1f).

The high quality of the Si replica is exhibited in Figure 3, with Figures 3a,b showing top and cross-sectional views, respectively. As the FIB cutting angle in Figure 3b was not perfectly parallel to the rods, it presents a cross-section through different parts of the rods. As expected when Si is deposited on the inner surfaces and therefore continually narrows the precursor's access channels, variations in the rod diameter can create occlusions and incomplete infiltration. Remaining air cavities in the wider parts are visible in Figure 3b and allow for a rough estimate of the rod filling fraction. Figures 3c,d present a side-by-side comparison of the Si woodpile with the original SU-8 structure. Note that even the surface roughness of the SU-8 woodpile, resulting from the finite resolution of the photoresist, is perfectly transferred into the Si structure.

A crucial test of the overall quality of any photonic crystal is optical-transmittance characterization. Due to the Cassegrain optics in our Fourier-transform spectrometer/microscope combination, the incident light spans an angle between 15° and 30° with respect to the surface normal for "normal incidence". The optical axis corresponds to the ΓX direction for face-centered-cubic symmetry. The photonic crystal transmittance is normalized to the transmittance of the bare sapphire substrate. The optical spectrum of the a-Si:H woodpile shows near-unity transmittance on the long-wavelength side and a

 © 2006 WILEY-VCH Verlag GmbH & Co. KGaA, Weinheim

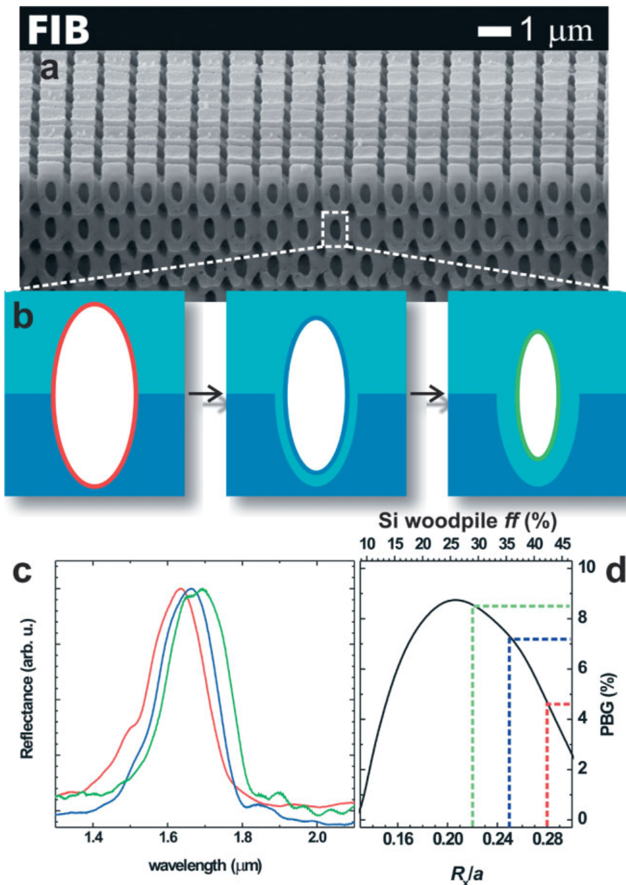

Figure 2. Fine-tuning of the rod filling fraction. a) SEM image of the FIB cross-section of the SiO_2 inverse woodpile showing the complete and uniform infiltration throughout the structure. b) Schematic representation of the sequential adjustment of the air filling fraction by SiO_2 CVD. c) Normalized reflectance spectra of the SiO_2 inverted woodpile before re-infiltration with SiO_2 (red, $ff = 42\,\%$, $a = 940$ nm, $R_x/a = 0.28$), after the first air filling fraction adjustment (blue, $ff = 34\,\%$, $a = 940$ nm, $R_x/a = 0.25$), and after the second air filling fraction adjustment (green, $ff = 27\,\%$, $a = 940$ nm, $R_x/a = 0.22$). d) Evolution of the calculated complete PBG width for the Si replica woodpile (80 % Si infiltration of the rods assumed, $n_{eff} = 3.16$).

prominent suppression of more than two orders of magnitude at a wavelength of 2.35 μm (Fig. 4c). Corresponding band structure calculations[22] with parameters taken from the SEM images reveal a complete PBG of 8.6 % ($a = 940$ nm, $ff = 27\,\%$, $R_x/a = 0.22$) (Fig. 4b). The refractive index of an a-Si:H thin film deposited under the same conditions has independently been measured as $n_{Si} = 3.7$. From the position and width of the complete PBG, we can estimate the effective refractive index of the rods as $n_{eff} = 3.16$, which is equivalent to a mixture of 80 % Si and 20 % air. This is in agreement with the images shown in Figure 3b. Improved control of the rod diameter in the original template might even allow for smaller air inclusions,[23] approaching a maximum gap of 12.9 % for complete Si infiltration ($n_{eff} = n_{Si} = 3.7$) (Fig. 4a). Further reducing the lattice constant of the template should allow for complete PBGs at telecommunication wavelengths.

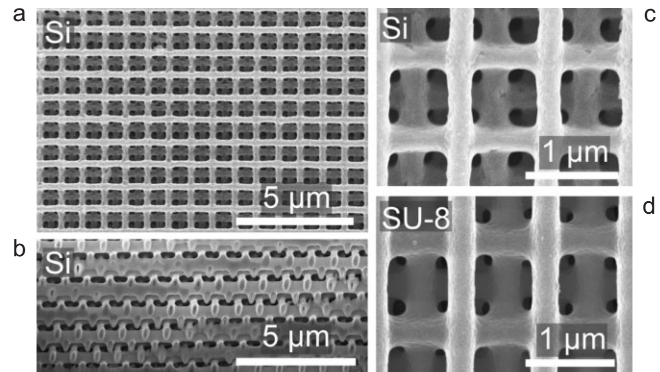

Figure 3. SEM image of an a-Si:H woodpile fabricated using the silicon double-inversion method: a) Top surface view, b) FIB cross-section showing complete and uniform infiltration of Si; c,d) side-by-side comparison of the Si replicate woodpile and the original SU-8 woodpile, respectively. Note the high-quality replication and the similar surface roughness.

In conclusion, silicon double inversion is a facile, versatile, and scalable method for the fabrication of high refractive index contrast replicas of 3D polymer templates made by direct laser writing, holographic laser lithography, or combinations thereof. These can include functional elements like point and line defects which would be perfectly replicated without additional steps. The fabrication of complex 3D photonic crystals with a complete PBG, like woodpile, slanted-pore,[14] square-spiral,[15,24] diamond-like, gyroid-like, and cubic structures,[10] is now possible with one method. Additionally, our approach allows for precise control of the filling fraction to fine-tune the complete PBG. This opens the door for rapid prototyping of novel 3D photonic architectures.

Experimental

For a detailed description of the fabrication of the polymer templates, we refer the interested reader to our previous publication [13].

Room-Temperature, Atmospheric-Pressure SiO_2 CVD: First, after an initial flushing of the deposition chamber for more than 30 min with N_2, the N_2 flow of 300 sccm is directed through a bubbler filled with twice-distilled H_2O for 7 min, leading to a physisorbed water layer on the sample surfaces. Subsequently, the chamber is flushed with N_2 for 5 min. Then, the N_2 flow is directed for 10 min through a bubbler containing $SiCl_4$ (Sigma–Aldrich 13736, > 99 %), which leads to the layer-by-layer growth of approximately 15–25 nm of dense, amorphous SiO_2 on the sample surfaces while releasing HCl. This sequence is repeated (on average 10–12 times) until the woodpile is completely infiltrated.

Reactive-Ion Etching: The SiO_2 overlayer is removed by RIE in an SF_6 plasma (15–30 min, 22 mtorr (1 torr ~ 133 Pa), 70 W forwarded power, 40 sccm SF_6, Oxford Plasmalab 80 Plus RIE system).

Removal of SU-8: SU-8 is removed by O_2 plasma etching ($t > 20$ h, Harrick PDC-3XG plasma cleaner/sterilizer, radio frequency power level approx. 5.4 W) or via calcination in air at 450 °C ($t > 6$ h, tube furnace Carbolite MTF 12/38/400).

Silicon CVD: For the silicon CVD, the silica-inverse woodpile is slowly ($t > 6$ h) heated to the deposition temperature of 460 °C. We use disilane (Si_2H_6) (Linde disilane 4.8) as a precursor. For the deposition, we flow 1 sccm disilane for 40 min at 3.26 mbar.

© 2006 WILEY-VCH Verlag GmbH & Co. KGaA, Weinheim

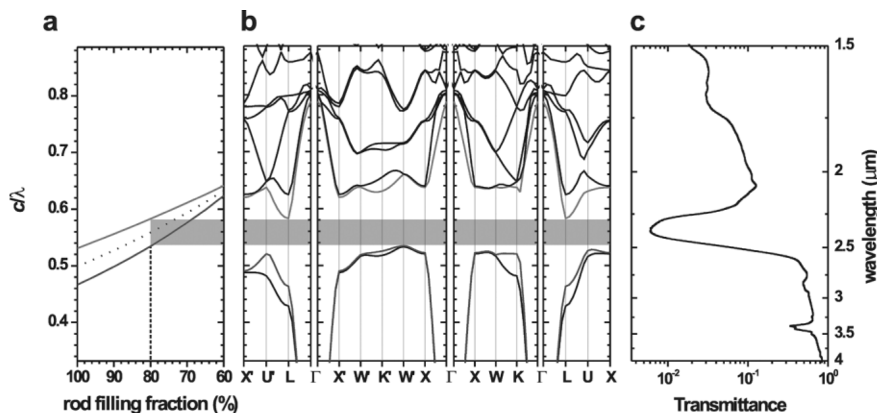

Figure 4. a–c) Experimental and theoretical properties of the Si woodpile. Comparison between measured transmittance (c) and a calculated band structure for parameters obtained from the SEM images (b) (a = 940 nm, ff = 27 %, R_x/a_{Si} = 0.22, n_{eff} = 3.16). The complete photonic bandgap is marked by the gray bar and corresponds to the transmittance dip in the experiment. Panel (a) shows the variation in gap width and position as a function of the Si infiltration efficiency in the rod (n_{eff} = 0.80 n_{Si} + 0.20 n_{air}, n_{Si} = 3.7).

SiO_2 Removal: A sapphire substrate is mounted on top of the sample with optical adhesive (Norland Adhesive 82) and cured for 15 min under UV light. The adhesive is further cured for 12 h at 50 °C to fully polymerize. The SiO_2 substrate as well as the inverse-woodpile is removed by wet chemical etching in 2 vol.-% aqueous HF for $t > 30$ h.

Optical Characterization: Measurements on the a-Si:H woodpile have been taken using a near-IR Fourier-transform interferometer (Bruker Equinox 55, NIR halogen source) connected to a microscope (Bruker Hyperion 1000, 36 × Cassegrain lens, numerical aperture $NA = 0.5$, liquid N_2-cooled InSb detector).

Received: August 10, 2005
Final version: August 26, 2005
Published online: October 11, 2005

[1] S. John, *Phys. Rev. Lett.* **1987**, *58*, 2486.
[2] E. Yablonovitch, *Phys. Rev. Lett.* **1987**, *58*, 2059.
[3] S. Y. Lin, J. G. Fleming, D. L. Hetherington, B. K. Smith, R. Biswas, K. M. Ho, M. M. Sigalas, W. Zubrzycki, S. R. Kurtz, J. Bur, *Nature* **1998**, *394*, 251.
[4] S. Noda, K. Tomoda, N. Yamamoto, A. Chutinan, *Science* **2000**, *289*, 604.
[5] K. Aoki, H. T. Miyazaki, H. Hirayama, K. Inoshita, T. Baba, K. Sakoda, N. Shinya, Y. Aoyagi, *Nat. Mater.* **2003**, *2*, 117.
[6] A. Blanco, E. Chomski, S. Grabtchak, M. Ibisate, S. John, S. W. Leonard, C. Lopez, F. Meseguer, H. Míguez, J. P. Mondia, G. A. Ozin, O. Toader, H. M. van Driel, *Nature* **2000**, *405*, 437.
[7] Y. A. Vlasov, X. Z. Bo, J. C. Sturm, D. J. Norris, *Nature* **2001**, *414*, 289.
[8] H. Míguez, N. Tétreault, S. M. Yang, V. Kitaev, G. A. Ozin, *Adv. Mater.* **2003**, *15*, 597.
[9] M. Campbell, D. Sharp, M. Harrison, R. Denning, A. Turberfield, *Nature* **2000**, *404*, 53.
[10] Y. V. Miklyaev, D. C. Meisel, A. Blanco, G. von Freymann, K. Busch, W. Koch, C. Enkrich, M. Deubel, M. Wegener, *Appl. Phys. Lett.* **2003**, *82*, 1284.
[11] H. B. Sun, S. Matsuo, H. Misawa, *Appl. Phys. Lett.* **1999**, *74*, 786.
[12] S. Kawata, H. B. Sun, T. Tanaka, K. Takada, *Nature* **2001**, *412*, 697.
[13] M. Deubel, G. von Freymann, M. Wegener, S. Pereira, K. Busch, C. M. Soukoulis, *Nat. Mater.* **2004**, *3*, 444.
[14] M. Deubel, M. Wegener, A. Kaso, S. John, *Appl. Phys. Lett.* **2004**, *85*, 1895.
[15] K. K. Seet, V. Mizeikis, S. Matsuo, S. Juodkazis, H. Misawa, *Adv. Mater.* **2005**, *17*, 541.
[16] M. Deubel, M. Wegener, S. Linden, G. von Freymann, *Appl. Phys. Lett* **2005**, unpublished.
[17] R. Hillebrand, U. Gösele, *Science* **2004**, *305*, 187.
[18] H. B. Sun, V. Mizeikis, Y. Xu, S. Juodkazis, J. Y. Ye, S. Matsuo, H. Misawa, *Appl. Phys. Lett.* **2001**, *79*, 1.
[19] K. Ho, C. Chan, C. Soukoulis, R. Biswas, M. Sigalas, *Solid State Commun.* **1994**, *89*, 413.
[20] H. Míguez, N. Tétreault, B. Hatton, S. M. Yang, D. Perovic, G. A. Ozin, *Chem. Comm.* **2002**, 2736.
[21] N. Tétreault, H. Míguez, S. M. Yang, V. Kitaev, G. A. Ozin, *Adv. Mater.* **2003**, *15*, 1167.
[22] S. G. Johnson, J. D. Joannopoulos, *Opt. Express* **2001**, *8*, 173.
[23] We would like to note that to date the achievable minimum feature size is mainly dominated by imperfections due to shrinkage during the SU-8 development process and due to the resolution of the photoresist. To date, samples fabricated via DLW could successfully reach a rod spacing of 650 nm [13]. Preliminary results on double inversion of samples fabricated via holographic lithography with minimum feature sizes of 100 nm were also reported by us: D. C. Meisel, K. Busch, M. Wegener, presented at PECS-VI, Int. Symp. on Photonic and Electromagnetic Crystal Structures, Aghia Pelaghia, Crete, Greece, June 2005.
[24] O. Toader, S. John, *Science* **2001**, *292*, 1133.

© 2006 WILEY-VCH Verlag GmbH & Co. KGaA, Weinheim